Role of redox signaling regulation in propyl gallate-induced apoptosis of human leukemia cells

Ching-Hsein Chen [a,*], Wan-Chen Lin [a], Chien-Neng Kuo [b,c], Fung-Jou Lu [d]

[a] Department of Microbiology, Immunology and Biopharmaceuticals, College of Life Sciences, National Chiayi University, Chiayi City 60004, Taiwan, ROC
[b] Department of Ophthalmology, Chang Gung Memorial Hospital, Chiayi, Taiwan, ROC
[c] Chang Gung University College of Medicine and Chang Gung Institute of Technology, Taiwan, ROC
[d] Department of Applied Chemistry, Chung Shan Medical University, Taichung 402, Taiwan, ROC

ARTICLE INFO

ABSTRACT

Propyl gallate (PG) is a synthetic antioxidant that has been used in processed food and medicinal preparations. The anti-cancer effect of PG in leukemia is unclear. In the present study, we demonstrate that PG reduced cell viability in THP-1, Jurkat, and HL-60 leukemia cells and induced apoptosis in THP-1 cells. PG activated caspases 3, 8, and 9 and increased the levels of p53, Bax, Fas, and Fas ligand. PG activated mitogen-activated protein kinases (MAPKs), inhibited nuclear translocation of the nuclear factor erythroid 2-related factor 2 (Nrf-2) and induced intracellular glutathione (GSH) depletion. In addition, PG increased superoxide dismutase-1 expression and decreased intracellular levels of reactive oxygen species. Our data show for the first time that an early event of PG-induced apoptosis is MAPKs/Nrf-2-mediated GSH depletion and that PG induced apoptosis via multiple pathways in human leukemia. PG might serve as a potential chemotherapeutic agent or food supplement for human leukemia patients.

Crown Copyright © 2010 Published by Elsevier Ltd. All rights reserved.

1. Introduction

Propyl gallate (PG), an ester also known as propyl 3,4,5-trihydroxybenzoate that belongs to the polyphenolic compound family, is synthesized by the condensation of propanol and gallic acid. PG has been proposed to act as an antioxidant that protects against oxidation by hydrogen peroxide and oxygen free radicals in foods containing oils and fats. This chemical is used in foods, cosmetics, hair products, adhesives, and lubricants. Aside from its antioxidant activity, the anticancer effects of PG have been noted in various human malignancies, including HeLa cervical cancer cells. Previous research suggests that PG inhibits the growth of HeLa cells by depleting intracellular glutathione (GSH) levels and inducing a G_1 phase arrest of the cell cycle. PG also changes the redox characteristics of HeLa cells by increasing the production of reactive oxygen species (ROS) and the activities of superoxide dismutase (SOD) and catalase (Han and Park, 2009). The GSH depletion-mediated apoptosis and ROS production induced by PG in HeLa cells also correlate with the activation of caspases 3, 8, or 9 (Han et al., 2009). However, while PG has a proven chemotherapeutic effect on HeLa cells, its general anti-cancer effects and the detailed mechanism through which redox signaling regulates the effect of PG on human leukemia cells remain unknown.

Intracellular GSH, a principal nonprotein thiol responsible for maintaining intracellular redox homeostasis, is an important antioxidant and cofactor for glutathione S-transferase conjugation. In most mammalian cells, intracellular GSH is synthesized by the sequential action of two enzymes, γ-glutamylcysteine synthetase (γ-GCS) and GSH synthetase. γ-GCS is the rate-limiting enzyme in the de novo synthesis of GSH, and γ-GCS regulation is one of the major determinants of GSH homeostasis (Li et al., 2010). γ-GCS is produced by phase II genes, which encode a series of enzymes necessary for the antioxidation and detoxification of endogenous and xenobiotic reactive and electrophilic compounds (Talalay et al., 2003). Transcriptional control of phase II genes is regulated by the binding of nuclear factor erythroid 2-related factor (Nrf-2) to consensus antioxidant response element sequences in the promoter regions. Activation of this pathway may offer potent and prolonged downstream antioxidant effects, including

elevated γ-GCS and SOD expression (Gao et al., 2001; Ha et al., 2006). To our knowledge, no study has thoroughly examined the ability of PG to affect Nrf-2 levels, which are believed to be a critical site of GSH depletion in human leukemia cells.

The mitogen-activated protein kinases (MAPKs), a family of highly related kinases, consist of the extracellular signal-regulated protein kinases (ERKs), the c-jun N-terminal kinases (JNKs), the p38 kinases and other relatively less characterized kinases, all of which catalyze phosphorylation on either threonine or serine residues adjacent to proline residues. The MAPK signaling system is susceptible to various stimuli, including oxidative stress, and has been associated with Nrf-2 regulation in many previous reports (McCubrey et al., 2006; Owuor and Kong, 2002; Sun et al., 2009). MAPK activation is also associated with the apoptosis induced by many anti-cancer agents. For example, ceramide results in p38 MAPK-dependent apoptosis in HL-60 human leukemia cells (Kim et al., 2008). Fenretinide stimulates sustained activation of JNK/p38 MAPK and apoptosis in a reactive oxygen species-dependent manner in neuroblastoma cells (Osone et al., 2004). The precise role of MAPKs and other molecular pathways involved in PG-induced apoptosis in human leukemia cells remain poorly understood.

The aim of this study was to evaluate the anti-cancer effects of PG on two well-characterized human acute myeloid leukemia cell lines, THP-1 and HL-60 cells, and one human T cell lymphoblast-like cell line, Jurkat cells. The relationship between GSH depletion, nuclear Nrf-2 translocation, and MAPK activation was investigated. Our results demonstrate that PG induces a MAPK activation-dependent reduction in Nrf-2 nuclear translocation and subsequent γ-GCS inhibition that ultimately results in GSH depletion. These results may be helpful in understanding the early apoptotic events in PG-treated leukemia cells.

2. Materials and methods

2.1. Cell lines and reagents

Three human leukemia cell lines, THP-1, HL-60, and Jurkat cells, were obtained from the Bioresource Collection and Research Center (Hsinchu, Taiwan). Chloromethylfluorescein diacetate (CMF-DA) was acquired from Invitrogen Co. (Carlsbad, CA). RPMI-1640 medium and fetal bovine serum (FBS) were obtained from Hyclone (South Logan, UT) and Biological industries (South Logan, UT), respectively. The primary antibodies against caspases 3, 8 and 9, Bcl-2, Bax, p53, Fas, Fas-L, SOD-1, catalase, γ-GCS, SP-1, and Nrf-2 were obtained from Santa Cruz Biotechnology, Inc., (Santa Cruz, CA). The primary antibodies against p-JNK, JNK, p-ERK, ERK, p-p38 and p38 were acquired from Cell Signaling Technology (Boston, MA). SB203580, SP600125 and PD98059 were purchased from Serva Electrophoresis (Mannheim, Germany). PG, propidium iodide (PI), NAC, GSH, 2′,7′-dichlorodihydrofluorescein-diacetate (DCFH-DA), 3-(4,5-dimethylthiazol-2-yl)-2,5-diphenyl tetrazolium bromide (MTT), DNase-free RNase A, dimethyl sulfoxide (DMSO), anti-actin primary antibody and other chemicals were purchased from Sigma Chemical Co. (St. Louis, MO).

2.2. Cell culture and treatment

THP-1, HL-60, and Jurkat cells were cultured in RPMI-1640 medium containing 10% FBS. The stock solution of PG was dissolved in DMSO, and different concentrations (μM) were prepared in the RPMI-1640 medium.

2.3. Cell viability assays

Cell viability was evaluated by the MTT assay. Yellow MTT is reduced to purple formazan by dehydrogenase in the mitochondria of living cells. A solubilization agent such as DMSO is added to dissolve the insoluble purple formazan product into a colored solution. The absorbance of this colored solution can be quantified by measuring a specific wavelength (usually between 550 and 600 nm) with a spectrophotometer. Cells (1×10^6) were cultured in 60 mm tissue-culture dishes for 24 h. The culture medium was replaced with new medium, and the cells were exposed to various concentrations of PG for the indicated times. After treatment, cells were incubated with 0.5 mg/mL of MTT reagent for 2 h and lysed with DMSO. A 200 μl

aliquot of DMSO lysed solution was taken from 60 mm culture-dishes to 96-well reader plates. The absorbance of DMSO lysed solution in 96-well reader plates was measured at 595 nm in a microplate reader (Bio-Rad, Richmond, CA).

2.4. DNA damage and cell cycle analysis

DNA damage and the cell cycle were measured with PI staining and flow cytometry. Cells (1×10^6) were cultured in 60 mm tissue culture dishes for 24 h. The culture medium was replaced with fresh medium, and the cells were exposed to various concentrations of PG for 24 h. After treatment, cells were pooled, washed with PBS, fixed in PBS-methanol (1:2, volume/volume) solution, and then maintained at 4 °C for at least 18 h. After one wash of PBS, the cell pellets were stained with the PI solution containing PBS, 40 μg/mL PI, and 40 μg/mL DNase-free RNase A for 30 min at room temperature in the dark and then analyzed by a Becton–Dickinson FACSan flow cytometer (Franklin Lakes, NJ). A minimum of 10,000 cells was counted per sample, and the DNA histograms were further evaluated using Modfit software on a PC workstation to calculate the percentage of cells in various phases of the cell cycle and to quantify cells with DNA damage.

2.5. Staining of apoptotic cells with Hoechst 33258 and apoptotic morphology analysis

After PG treatment, cells were washed with PBS and resuspended in PBS. One hundred microliters of cell suspension (1×10^6 cells) were incubated with 50 μM Hoechst 33258 for 10 min. Apoptotic cells displaying chromatin condensation were evaluated by fluorescence microscopy. Apoptotic morphology indicated by apoptotic bubbling was examined with a light microscope.

2.6. Measurement of intracellular ROS by flow cytometry

Production of intracellular ROS was detected by flow cytometry using DCFH-DA. After treatment, cells were washed once with PBS, treated with 20 μM DCFH-DA for 30 min in the dark, washed once with PBS, collected by centrifugation, and suspended in PBS. Intracellular ROS levels, as indicated by the fluorescence of dichlorofluorescein (DCF), were measured through a 530/22-nm barrier filter using a Becton–Dickinson FACS-Calibur flow cytometer.

2.7. Measurement of intracellular GSH depletion

After treatment, cells were incubated with 25 μM CMF-DA for 20 min at 37 °C in a 5% CO_2 incubator, washed once with PBS, collected by centrifugation, suspended in PBS, and then measured through a 530/22-nm barrier filter using a Becton–Dickinson FACSan flow cytometer. The CMF fluorescence gives a measure of the intracellular GSH level.

2.8. Preparation of nuclear extracts for Nrf-2

Cells (3×10^6) were washed with cold PBS and suspended in 0.15 ml of hypotonic lysis buffer containing protease inhibitors for 30 min. The cells were then lysed with 3.2 μl of 10% Nonidet P-40. The homogenate was centrifuged, and the supernatant containing the cytoplasmic extracts was stored frozen at −80 °C. The nuclear pellet was resuspended in a 25 μl of ice-cold nuclear extraction buffer. After 30 min of intermittent mixing, the extract was centrifuged, and the supernatants containing nuclear extracts were secured. Protein content was measured with the Bio-Rad protein assay reagent. The expression of Nrf-2 was measured by western blotting.

2.9. Western blotting analysis

After treatment, cells were washed with PBS, resuspended in a protein extraction buffer for 10 min, and centrifuged at 12,000g for 10 min at 4 °C to obtain total extracted proteins (supernatant). Protein concentrations were measured with a Bio-Rad protein assay reagent (Bio-Rad, Richmond, CA). The extracted cellular proteins were boiled in loading buffer, and an aliquot corresponding to 50–100 μg of protein was separated on a 12% SDS–polyacrylamide gel. After electrophoresis, proteins were electrotransferred onto a polyvinylidene fluoride transfer membrane. After blotting, the membranes were incubated with various primary antibodies overnight and then washed with PBST solution (0.05% Tween 20 in PBS). Following washing, the secondary antibody labeled with horseradish-peroxidase was added to the membrane for 1 h and then washed with PBST solution (0.05% Tween 20 in PBS). The antigen–antibody complexes were detected by enhanced chemiluminescence (Amersham Pharmacia Biotech, Piscataway, NJ) with a chemiluminescence analyzer.

2.10. Statistical analysis

Data are presented as the means ± standard deviation from at least three independent experiments and were analyzed using Student's t-test. A P value of less than 0.05 was considered statistically significant (Lucke, 1996).

3. Results

3.1. PG induces apoptosis in THP-1 cells but not in HL-60 cells or Jurkat cells

Treatment of three leukemia cell lines, THP-1, HL-60 and Jurkat cells, with PG (0, 5, 10, 25, 50, or 75 μM) resulted in a dose-dependent decrease in cell viability as measured by the MTT assay (Fig. 1A). To evaluate whether PG induced apoptosis, these human leukemia cells were exposed to 75 μM PG for 24 h. The apoptotic-associated DNA damage fraction ($SubG_1$) was evaluated by PI staining and flow cytometry, and apoptotic bubbling and chromatin condensation were examined with a light microscope and Hoechst 33258 staining, respectively. As shown in Fig. 1B, the proportion of

THP-1 cells in $SubG_1$ increased to 48.84% after a 24-h PG treatment. Treatment with PG for 24 h had almost no effect on $SubG_1$ levels in HL-60 cells and Jurkat cells. In agreement with the DNA damage level, PG-induced marked apoptotic bubbling and chromatin condensation in THP-1 but not in HL-60 or Jurkat cells (Fig. 1C and D). Because PG induced the greatest level of apoptosis in THP-1 cells, the proportion of cells in $SubG_1$ was further evaluated in this cell line at various concentrations of PG. For treatments lasting 24 h, increasing concentrations of PG caused a progressive increase in the proportion of cells in $SubG_1$ (Fig. 1E). We also evaluated the effect of PG treatment on the cells viability in two normal human cell lines (WI-38 and ARPE-19). WI-38 is a normal human lung cell line and ARPE-19 is a normal human retinal pigment epithelial cell line. As shown in Fig. 1F, WI-38 and ARPE-19 cells were treated
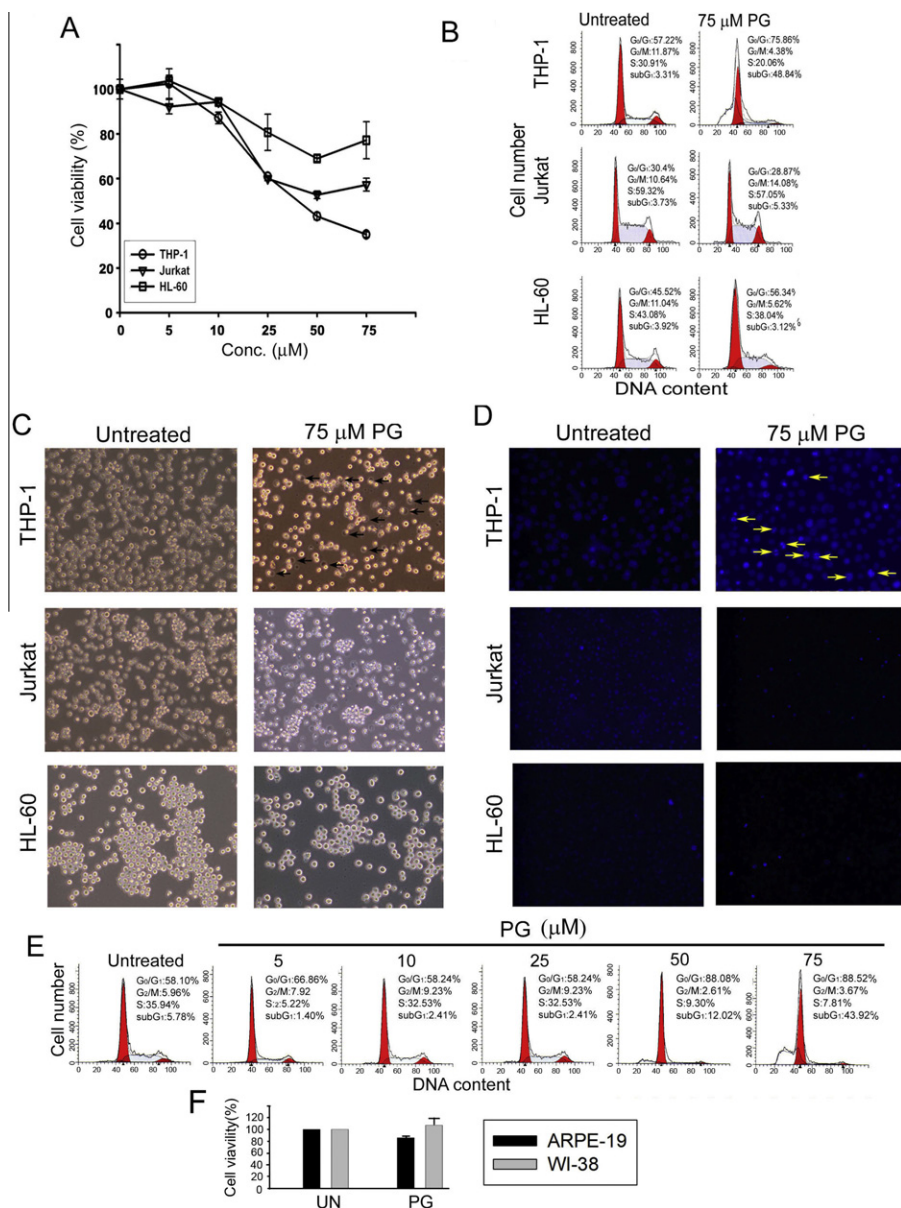

Fig. 1. Cell viability and apoptosis analysis in PG-treated leukemia, WI-38, and ARPE-19 cell lines. THP-1, Jurkat, HL-60, WI-38, and ARPE-19 cells were plated in 60-mm culture dishes at 80% confluence and treated with the indicated concentrations for 24 h. (A) and (F) After treatment, the MTT reagent (0.5 mg/ml) was added to the cells for 2 h at 37 °C, and the cells were lysed with DMSO. Absorbance was measured at 595 nm. (B) and (E) After treatment, cells were harvested, fixed in PBS-methanol (1:2, volume/volume) solution, and stained with propidium iodide, followed by flow cytometric analysis. (C) After treatment, apoptotic morphology was evaluated with a light microscope (magnification 200×). The arrows indicate apoptotic bubbles. (D) After treatment, the cells were stained with Hoechst 33258, and chromatin condensation was evaluated with a fluorescence microscope (magnification 200×). The arrows indicate the chromatin condensation in cells.

with PG for 24 h, resulting in 109.9% and 85.6% cells viability, respectively. There is little or none toxicity in PG-treated normal cells at the test conditions.

3.2. PG induces caspase activation, Bax and p53 expression in THP-1 cells

Because caspase activation is thought to induce apoptosis, and up-regulation of Bax, Bcl-2, and p53 is an important event in the apoptosis process, we examined whether PG mediated the cleavage of caspases 3, 8, and 9 or affected Bax, Bcl-2 or p53 levels in treated THP-1 cells. As shown in Fig. 2A, the cleavage of caspases 3, 8, and 9 was markedly increased at 6, 12, and 24 h in PG-treated cells compared with untreated cells. PG treatment induced an increase in Bax expression that was clearly visible after 12 and 24 h of treatment (Fig. 2B); however, no significant change in Bcl-2 was apparent in treated THP-1 cells. The PG-treated THP-1 cells also exhibited an increase in p53 protein levels that was detectable after 6 h of treatment and maintained to the 24-h endpoint.

3.3. PG induces intracellular GSH depletion but not ROS production in THP-1 cells

GSH depletion and ROS production are two important events in the apoptotic process. Because PG has been shown to induce a GSH decrease and ROS increase in human cervical cancer HeLa cells in another study (Han and Park, 2009), we assessed whether PG treatment also affected GSH and ROS levels in THP-1 cells. As shown in Fig. 3A, the percentage of intracellular GSH-depleted cells in-

creased slightly to 7.7 ± 2.8 and 9.5 ± 3.5 after 3 and 6 h of treatment, respectively, compared to untreated cells. After 24 h of treatment, the percentage of intracellular GSH-depleted cells increased to 23.6 ± 5.8. Intracellular ROS levels, as indicated by DCF fluorescence, were reduced upon PG treatments of various durations (Fig. 3B). These results indicate that the GSH depletion induced by PG is not dependent on intracellular ROS production.

3.4. PG decreases Nrf-2 nuclear translocation and γ-GCS expression in THP-1 cells

γ-GCS is the rate-limiting enzyme for GSH synthesis and is transcriptionally regulated by the transcription factor Nrf-2. To gain further insight into the mechanism of PG-mediated GSH depletion, we determined its effect on Nrf-2 nuclear translocation and γ-GCS expression in THP-1 cells by western blotting. As shown in Fig. 4A, the Nrf-2 nuclear fraction was decreased as early as 0.5 h after onset of PG treatment, and maintained low 3 h later. γ-GCS expression in PG-treated THP-1 cells declined in a time-dependent manner (Fig. 4B). Because SOD and catalase are two important intracellular antioxidants that scavenge superoxide and H_2O_2, respectively, we next determined whether the PG-induced ROS reduction was associated with either enzyme. As shown in Fig. 4B, the expression of SOD-1 in PG-treated THP-1 cells increased in a time-dependent manner, but catalase expression was not affected by PG treatment.

3.5. PG induces MAPK activation and Fas and Fas ligand expression in THP-1 cells

Previous studies have shown that MAPK activation is a critical event for the induction of apoptosis (Lau et al., 2010). To determine whether PG enhances MAPK activation, the phosphorylation of JNK, ERK, and p38 was measured by western blotting. As shown in Fig. 4C, JNK, ERK, and p38 each showed a transient rise in phosphorylation at 10 min, which decreased at later time points. Fas has been shown to be an important mediator of apoptotic cell death and activation of Fas by Fas ligand (Fas-L) induces apoptosis (Miyata et al., 2010). We therefore determined the expression of Fas and Fas-L in PG-treated THP-1 cells by western blotting. As shown in Fig. 4D, a marked increase in Fas expression was observed at 6, 12 and 24 h after PG treatment. A significant increase in Fas-L level, correlated with changes in Fas level, was detected at 12 h and 24 h.

3.6. PG-induced apoptosis in THP-1 cells through multiple pathways

To investigate the critical pathway(s) in PG-induced apoptosis, THP-1 cells were pretreated with 100 μM Boc-Asp(OMe)-fmk (a pan caspase inhibitor), 100 μM pifithrin-α (a p53 inhibitor), 10 mM NAC (an intracellular GSH synthetic agent), 20 μM SB203580 (a p38 inhibitor), 20 μM SP600125 (a JNK inhibitor) or 20 μM PD98059 (a MEK inhibitor) for 2 h, followed by treatment with 75 μM PG for another 24 h. The SubG$_1$ fraction was then analyzed by PI staining and flow cytometry. As shown in Fig. 5A, the SubG$_1$ fraction in untreated THP-1 cells was 0.37% and increased to 45.22% after 24 h of exposure to 75 μM PG. Boc-Asp(OMe)-fmk pretreatment rescued PG-induced apoptosis to the greatest extent: the percentage of SubG$_1$ cells decreased to 8.43% in these cells. Pifithrin-α and NAC displayed moderate inhibitory effects, with respective SubG$_1$ fractions of 23.81% and 26.67%. Regarding the MAPK inhibitor pretreatments, PD98059 reduced the SubG$_1$ fraction to 18.02% after 24 h of treatment, compared to 51.19% in the PG-treated cells (Fig. 5B). SB203580 displayed a moderate effects; the SubG$_1$ fraction in these cells was 46.48%. SP600125 had the weakest effect on PG-induced apoptosis, as cells pre-treated with
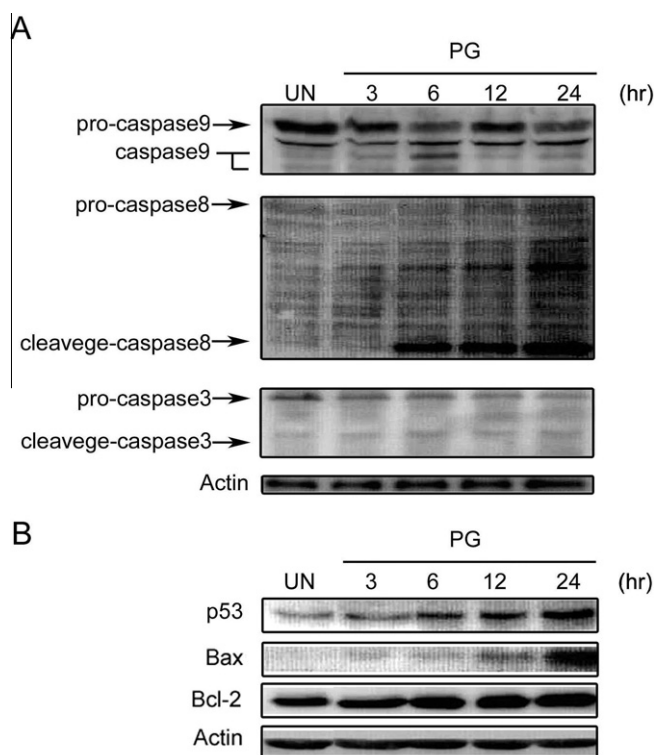

Fig. 2. (A) Activation of caspases 3, 8, and 9 and (B) the expression of p53, Bax, and Bcl-2 in PG-treated THP-1 cells. Cells were plated in 60-mm culture dishes at 80% confluence and then treated with 75 μM PG for 3, 6, 12 or 24 h. After treatment, cells were washed with PBS and extracted with protein extraction buffer. Fifty micrograms of protein were loaded on a 12% SDS–polyacrylamide gel and evaluated by western blotting. These experiments were performed at least three times and a representative experiment is presented.
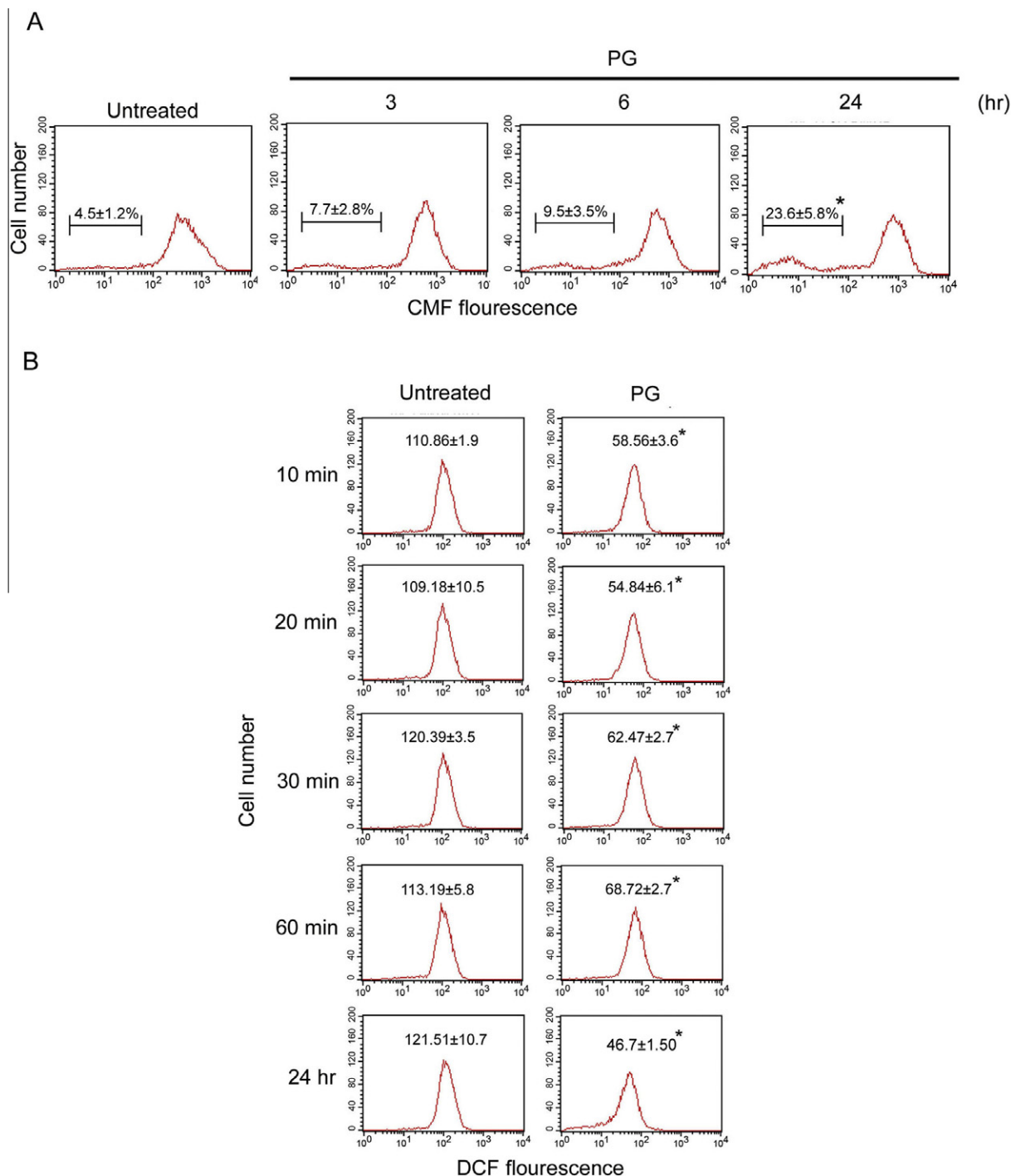
Fig. 3. Evaluation of intracellular GSH and ROS in PG-treated THP-1 cells. Cells were plated in 60-mm culture dishes. (A) The culture medium was replaced with fresh medium when the cells were 80% confluent and then treated with 0 (untreated) or 75 μM of PG for 3, 6, or 24 h. After treatment, the cells were incubated with 25 μM CMF-DA for 30 min in a 37 °C 5% CO_2 incubator and then measured with a flow cytometer. Data show the percentage of intracellular GSH-negative cells. (B) The culture medium was replaced with fresh medium when the cells were 80% confluent and then exposed to 75 μM of PG for 10, 20, 30, 60 min, or 24 h. Production of intracellular ROS was detected by flow cytometry using DCFH-DA staining. The intracellular fluorescence of dichlorofluorescein (DCF) was measured with a Becton–Dickinson FACScan flow cytometer. Data in each panel represent the DCF fluorescence intensity within the cells. The values shown are mean ± standard deviation ($n = 5$–8 samples per experiment). Significant differences from the untreated group show $P < 0.05$ (∗).

this inhibitor displayed a SubG$_1$ fraction of 35.61%. These results indicate that the apoptotic effect induced by PG in THP-1 cells is mediated by multiple pathways. To evaluate whether MAPK activation inhibits Nrf-2 nuclear translocation, THP-1 cells were pretreated with 20 μM SB203580, 20 μM SP600125 or 20 μM PD98059 for 2 h, followed by treatment with 75 μM PG for another 30 min. Nrf-2 nuclear translocation was then analyzed by western blotting. As shown in Fig. 5C, pretreatment with SB203580 or PD98059 rescued nuclear Nrf-2 accumulation in PG-treated cells, indicating that the PG-induced inhibition of Nrf-2 nuclear translocation depends on the activation of MEK/ERK and p38. Treatment of NAC to the THP-1 cells after treating with PG for 12 h does not
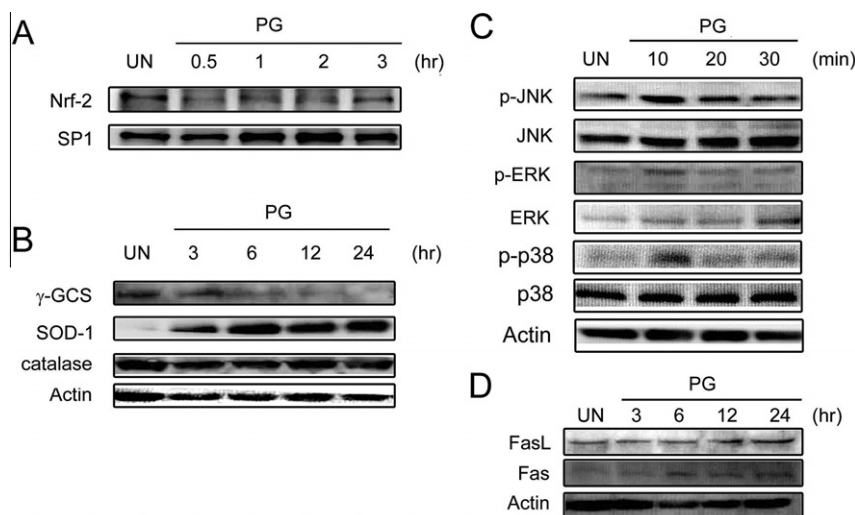
Fig. 4. (A) Nrf-2 nuclear translocation, (B) the expression of γ-GCS, SOD-1, and catalase, (C) Activation of JNK, ERK and p38, and (D) the expression of Fas-L and Fas in PG-treated THP-1 cells. Cells were plated in 60-mm culture dishes at 80% confluence and then treated with 75 μM PG for the indicated times. After treatment, nuclear proteins were isolated and examined for Nrf-2; total protein was extracted to assess γ-GCS, SOD-1, catalase, Fas-L and Fas expression and phosphorylation and non- phosphorylation of JNK, ERK and p38. Fifty micrograms of protein were loaded on a 12% SDS–polyacrylamide gel and evaluated by western blotting. These experiments were performed at least three times and a representative experiment is presented.

prevent the PG-induced apoptosis (Fig. 5D). PG also can not induce obvious apoptosis (<10%) at 3–12 h (Fig. 5E). These results indicate that GSH depletion is a consequence of cell death. Fig. 5F shows that 5 μM of SB203580 did not induce marked apoptosis in THP-1 cells. Other inhibitors or scavengers also did not induce obvious apoptotic effects on control cells (<10%).

4. Discussion

Many anti-cancer drugs kill cancer cells by inducing high levels of intracellular ROS. Some studies have suggested that high concentrations of PG (∼400 μM) induce increased ROS levels and cell death in HeLa human cervical cancer cells (Han and Park, 2009). However, our results show that 75 μM PG reduced intracellular ROS levels to about half that seen in untreated THP-1 cells at every time point (Fig. 3B). PG contains a hydrophobic alkyl ester group that helps PG to cross the cell membrane and enter the cytoplasm. Once in the cytoplasm, the hydroxyl groups on the polyphenolic structure of PG can scavenge free radicals by donating hydrogen atoms (Maisuthisakul et al., 2007). Another mechanism by which PG might decrease intracellular ROS is the up-regulation of SOD-1 observed in THP-1 cells after 3 h of treatment (Fig. 4B). SOD is a superoxide scavenger that metabolizes superoxide to H_2O_2, which is further metabolized to H_2O and O_2 by catalase. Because PG did not affect the expression of catalase (Fig. 4B), the elimination of intracellular H_2O_2 could be executed normally in THP-1 cells and ultimately contribute to the decrease in intracellular ROS in PG-treated THP-1 cells.

GSH depletion has been accepted as an important event for successful induction of apoptosis by various chemical compounds in many cancer cell lines. Our previous study demonstrated that GSH depletion occurs after treatment with several chemical compounds, including actinodaphnine, secokotomolide A and 6-shogaol, which induce some human cancer cell lines (Hsieh et al., 2006; Chen et al., 2006, 2007). PG did not induce intracellular ROS production, suggesting that GSH depletion is dependent on the inhibition of Nrf-2 nuclear translocation and γ-GCS expression rather than ROS production in PG-treated THP-1 cells (Fig. 4). Pretreatment with NAC partially decreased of the size of the SubG$_1$

fraction induced by PG (Fig. 5A), indicating that GSH depletion participated in the apoptotic process that follows PG treatment.

Previous studies recognized that the tumor suppressor p53 exerts its anti-neoplastic activity primarily through the induction of apoptosis, and that cytosolic localization of endogenous wild type p53 is necessary and sufficient for apoptosis (Chipuk et al., 2004). P53 can directly activate the proapoptotic Bax protein to permeabilize the mitochondria and activate the apoptotic program (Chipuk et al., 2004). Consistent with these observations, our data indicate that PG-induced p53 expression at 6–24 h and Bax expression at 12 and 24 h. In addition, we show that pretreatment with the p53 inhibitor pifithrin-α also decreased the percentage of SubG$_1$ cells to about half that measured in PG-treated cells. These results indicate that p53-dependent Bax induction may be an important pathway for apoptotic injury during PG exposure.

Caspase family proteins are some of the chief executors of the apoptotic process (Lampiasi et al., 2009). They belong to a class of enzymes known as cysteine proteases and are present within the cell as inactive zymogens. These zymogens can be cleaved and transformed into active enzymes following the induction of apoptosis. Apoptosis can be initiated via extrinsic death receptors or by intrinsic mitochondrial dysfunction, which result in the activation of caspases 8 and 9, respectively. These caspases then activate other caspases in a cascade that eventually leads to the activation of effector caspases such as caspase 3. Effector caspases are responsible for the cleavage of key cellular proteins that mediate apoptosis (Lampiasi et al., 2009). Our results show that caspases 8, 9, and 3 were activated by 6 h after the onset of PG treatment. Moreover, we demonstrated that Boc-Asp(OMe)-fmk (a pan caspase inhibitor) decreased the percentage of SubG$_1$ cells induced by PG, suggesting that caspase activation is the chief pathway involved in PG-mediated apoptosis.

Exposure of cells to oxidative stress induces activation of multiple members of the MAPK family, including ERK1/2, JNK, and p38 (Torres and Forman, 2003). Among them, the JNK and p38 pathways are frequently associated with the induction of apoptosis, while the ERK pathway is thought to deliver survival signals that protect cells from apoptosis (Yang et al., 2004). However, increasing evidence indicates that ERK activation results in apoptosis in certain cell types. For example, cisplatin induces ERK1/2 activation, and inhibition of ERK prevented apoptosis in renal epithelial cells
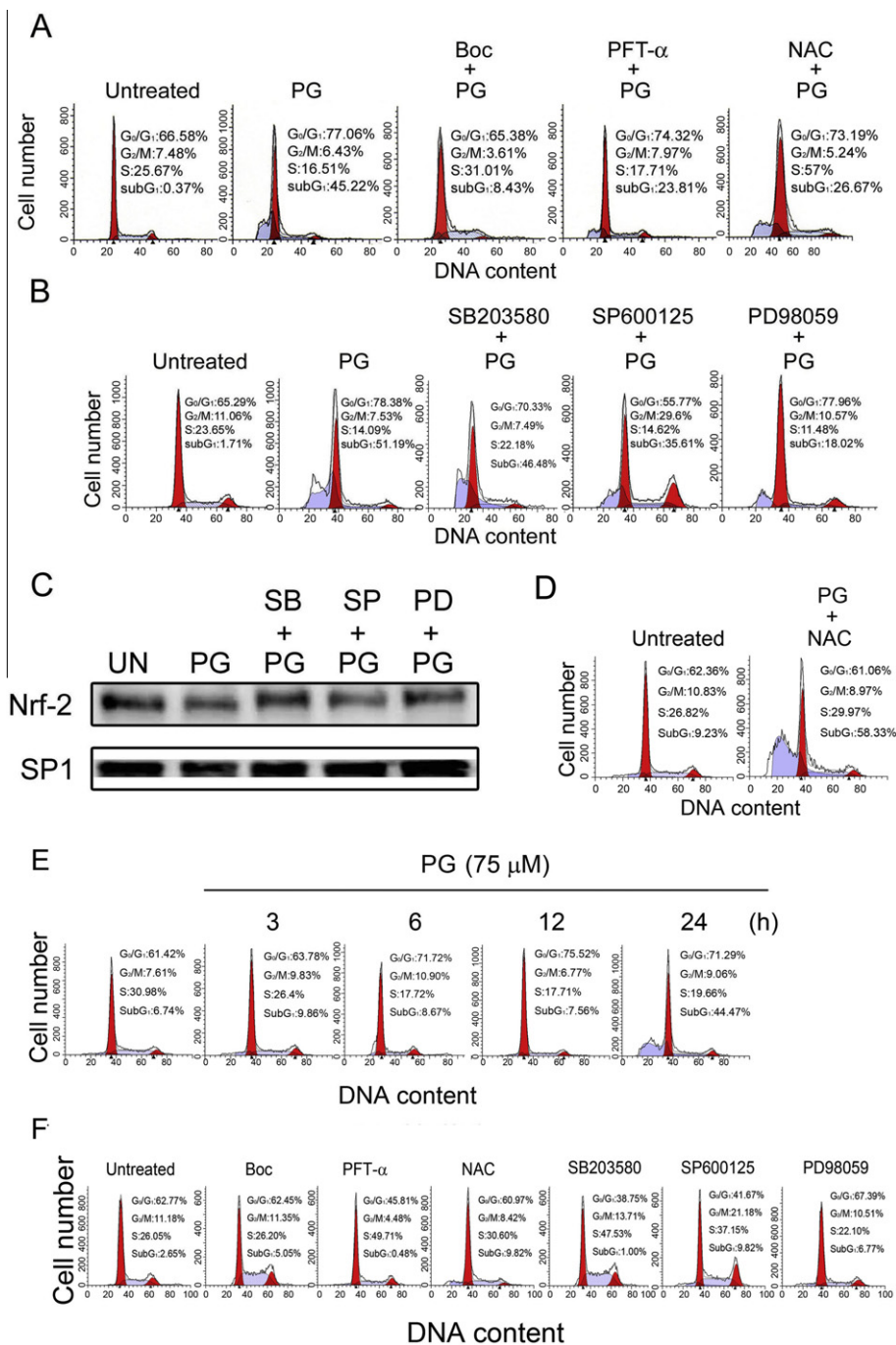
Fig. 5. Evaluation of critical events in PG-induced apoptosis. (A) THP-1 cells were treated with 0 (untreated) or 75 µM PG alone for 24 h, or pretreated with 100 µM Boc [Boc-Asp(OMe)-fmk], 100 µM PFT-α (pifithrin-α, or 10 mM NAC (N-acetylcysteine) for 2 h, followed by 75 µM PG treatment for 24 h. All samples were subsequently processed for cell cycle analysis. (B) THP-1 cells were treated with 0 (untreated) or 75 µM PG alone for 24 h, or pretreated with 5 µM SB203580, 20 µM SP600125 or 20 µM PD98059 for 2 h, followed by 75 µM PG treatment for 24 h. All samples were subsequently processed for cell cycle analysis. (C) THP-1 cells were treated with 0 (untreated) or 75 µM PG alone for 30 min, or pretreated with 20 µM SB203580 (SB), SP600125 (SP) or PD98059 (PD) for 2 h, followed by 75 µM PG treatment for 30 min. Nuclear proteins were isolated from each sample. Fifty micrograms of protein were loaded on a 12% SDS–polyacrylamide gel and the expression of Nrf-2 was evaluated by western blotting analysis. (D) THP-1 cells were treated with 10 mM NAC after treatment with 75 µM PG for 12 h. After 24 h of PG treatment, the cells were processed for cell cycle analysis. (E) THP-1 cells were treated with 75 µM PG for the indicated times; (F) THP-1 cells were treated with 100 µM Boc [Boc-Asp(OMe)-fmk], 100 µM PFT-α, 10 mM NAC, 5 µM SB203580, 20 µM SP600125 or 20 µM PD98059 for 24 h. After treatment, all samples were subsequently processed for cell cycle analysis. These experiments were performed at least three times and a representative experiment is presented.

(Kim et al., 2005). Moreover, ERK inhibition by U0126 resulted in renal protection in cisplatin-induced nephrotoxicity in mice (Jo et al., 2005). Although JNK, p38, and ERK activation were apparent as early as 10 min after the onset of PG treatment, inhibition of MEK by PD98059, a MEK inhibitor, resulted in the greatest reduction of PG-induced $SubG_1$ cells (Fig. 5B). This result indicates that

MEK/ERK signaling may be an early initiator of the PG-induced apoptotic process. Furthermore, another study also showed that activation of ERK contributed to Fas and Fas-L expression and the activation of caspase 8 (Chen et al., 2010). Our results show that up-regulation of Fas and Fas-L and caspase 8 activation may be two downstream events of MEK/ERK signaling in PG-treated
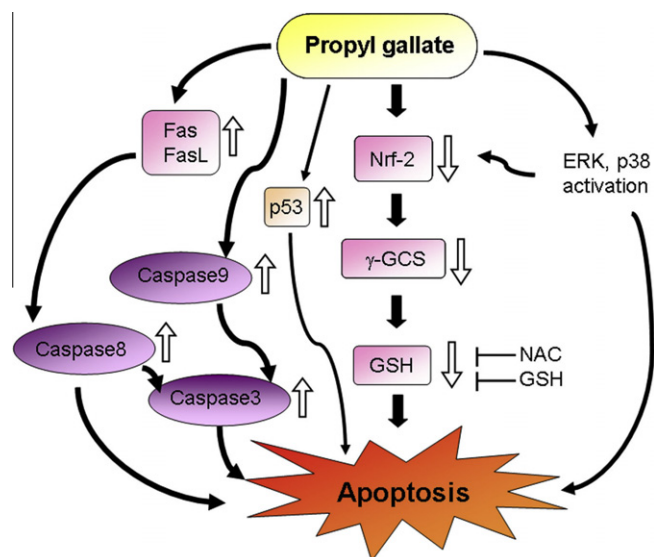
Fig. 6. Schematic illustration of a proposed model of PG-induced apoptosis in THP-1 cells.

THP-1 cells. These findings are in accordance with results from other studies that reported ERK activation accompanied by the Fas response in valproate-induced apoptosis in B-chronic lymphocytic leukaemia cells (Bouzar et al., 2009).

Our studies demonstrate for the first time that PG causes apoptosis in human leukemia cells via multiple pathways, including activation of caspases and MAPKs, up-regulation of p53, Bax, Fas, and Fas-L expression and GSH depletion. Among these pathways, caspase activation is the chief effect, with MAPK activation and p53 expression/GSH depletion as the second and third effects, respectively. The activation of MEK/ERK and MAPK/p38 is an early event in PG-induced inhibition of Nrf-2 nuclear translocation, which may result in γ-GCS down-regulation and GSH depletion. A hypothetical diagram that illustrates the apoptotic effects of PG on leukemia cells is depicted in Fig. 6. PG might serve as a potential chemotherapeutic agent or food supplement for human leukemia patients.

Conflict of Interest

The authors declare that there are no conflicts of interest.

Acknowledgements

References

Bouzar, A.B., Boxus, M., Defoiche, J., Berchem, G., Macallan, D., Pettengell, R., Willis, F., Burny, A., Lagneaux, L., Bron, D., Chatelain, B., Chatelain, C., Willems, L., 2009. Valproate synergizes with purine nucleoside analogues to induce apoptosis of B-chronic lymphocytic leukaemia cells. British Journal of Haematology 144, 41–52.

Chen, C.H., Lo, W.L., Liu, Y.C., Chen, C.Y., 2006. Chemical and cytotoxic constituents from the leaves of Cinnamomum kotoense. Journal of Natural Products 69, 927–933.

Chen, C.Y., Liu, T.Z., Liu, Y.W., Tseng, W.C., Liu, R.H., Lu, F.J., Lin, Y.S., Kuo, S.H., Chen, C.H., 2007. 6-Shogaol (alkanone from ginger) induces apoptotic cell death of human hepatoma p53 mutant Mahlavu subline via an oxidative stress-mediated caspase-dependent mechanism. Journal of Agricultural and Food Chemistry 55, 948–954.

Chen, K.C., Liu, W.H., Chang, L.S., 2010. Suppression of ERK signaling evokes autocrine Fas-mediated death in arachidonic acid-treated human chronic myeloid leukemia K562 cells. Journal of Cellular Physiology 222, 625–634.

Chipuk, J.E., Kuwana, T., Bouchier-Hayes, L., Droin, N.M., Newmeyer, D.D., Schuler, M., Green, D.R., 2004. Direct activation of Bax by p53 mediates mitochondrial membrane permeabilization and apoptosis. Science 303, 1010–1014.

Gao, X., Dinkova-Kostova, A.T., Talalay, P., 2001. Powerful and prolonged protection of human retinal pigment epithelial cells, keratinocytes, and mouse leukemia cells against oxidative damage: the indirect antioxidant effects of sulforaphane. Proceedings of the National Academy of Sciences of the United States of America 98, 15221–15226.

Ha, K.N., Chen, Y., Cai, J., Sternberg Jr., P., 2006. Increased glutathione synthesis through an ARE-Nrf2-dependent pathway by zinc in the RPE: implication for protection against oxidative stress. Investigative Ophthalmology & Visual Science 47, 2709–2715.

Han, Y.H., Park, W.H., 2009. Propyl gallate inhibits the growth of HeLa cells via regulating intracellular GSH level. Food Chemical Toxicology 47, 2531–2538.

Han, Y.H., Moon, H.J., You, B.R., Park, W.H., 2009. The anti-apoptotic effects of caspase inhibitors on propyl gallate-treated HeLa cells in relation to reactive oxygen species and glutathione levels. Archives of Toxicology 83, 825–833.

Hsieh, T.J., Liu, T.Z., Lu, F.J., Hsieh, P.Y., Chen, C.H., 2006. Actindaphnine induces apoptosis through increased nitric oxide, reactive oxygen species and down-regulation of NF-kappaB signaling in human hepatoma Mahlavu cells. Food and Chemical Toxicology 44, 344–354.

Jo, S.K., Cho, W.Y., Sung, S.A., Kim, H.K., Won, N.H., 2005. MEK inhibitor, U0126, attenuates cisplatin-induced renal injury by decreasing inflammation and apoptosis. Kidney International 67, 458–466.

Kim, H.J., Oh, J.E., Kim, S.W., Chun, Y.J., Kim, M.Y., 2008. Ceramide induces p38 MAPK-dependent apoptosis and Bax translocation via inhibition of Akt in HL-60 cells. Cancer Letters 18 (260), 88–95.

Kim, Y.K., Kim, H.J., Kwon, C.H., Kim, J.H., Woo, J.S., Jung, J.S., Kim, J.M., 2005. Role of ERK activation in cisplatin-induced apoptosis in OK renal epithelial cells. Journal of Applied Toxicology: JAT 25, 374–382.

Lampiasi, N., Azzolina, A., D'Alessandro, N., Umezawa, K., McCubrey, J.A., Montalto, G., Cervello, M., 2009. Antitumor effects of dehydroxymethylepoxyquinomicin, a novel nuclear factor-κB inhibitor, in human liver cancer cells are mediated through a reactive oxygen species-dependent mechanism. Molecular Pharmacology 76, 290–300.

Lau, S.T., Lin, Z.X., Leung, P.S., 2010. Role of reactive oxygen species in brucein D-mediated p38-mitogen-activated protein kinase and nuclear factor-kappaB signalling pathways in human pancreatic adenocarcinoma cells. British Journal of Cancer 102, 583–593.

Li, B., Li, L., Donaldson, P.J., Lim, J.C., 2010. Dynamic regulation of GSH synthesis and uptake pathways in the rat lens epithelium. Experimental Eye Research 90, 300–307.

Lucke, J.F., 1996. Student's t test and the Glasgow Coma Scale. Annals of Emergency Medicine 28, 408–413.

Maisuthisakul, P., Suttajit, M., Pongsawatmanit, R., 2007. Assessment of phenolic content and free radical-scavenging capacity of some Thai indigenous plants. Food Chemistry 100, 1409–1418.

McCubrey, J.A., Lahair, M.M., Franklin, R.A., 2006. Reactive oxygen speciesinduced activation of the MAP kinase signaling pathways. Antioxidants and Redox Signaling 8, 1775–1789.

Miyata, S., Takemura, G., Kosai, K., Takahashi, T., Esaki, M., Li, L., Kanamori, H., Maruyama, R., Goto, K., Tsujimoto, A., Takeyama, T., Kawaguchi, T., Ohno, T., Nishigaki, K., Fujiwara, T., Fujiwara, H., Minatoguchi, S., 2010. Anti-Fas gene therapy prevents doxorubicin-induced acute cardiotoxicity through mechanisms independent of apoptosis. The American Journal of Pathology 176, 687–698.

Osone, S., Hosoi, H., Kuwahara, Y., Matsumoto, Y., Iehara, T., Sugimoto, T., 2004. Fenretinide induces sustained-activation of JNK/p38 MAPK and apoptosis in a reactive oxygen species-dependent manner in neuroblastoma cells. Internal Journal of Cancer 112, 219–224.

Owuor, E.D., Kong, A.N., 2002. Antioxidants and oxidants regulated signal transduction pathways. Biochemical Pharmacology 64, 765–770.

Sun, Z., Huang, Z., Zhang, D.D., 2009. Phosphorylation of Nrf2 at multiple sites by MAP kinases has a limited contribution in modulating the Nrf2-dependent antioxidant response. PloS One 4, e6588.

Talalay, P., Dinkova-Kostova, A.T., Holtzclaw, W.D., 2003. Importance of phase 2 gene regulation in protection against electrophile and reactive oxygen toxicity and carcinogenesis. Advances in Enzyme Regulation 43, 121–134.

Torres, M., Forman, H.J., 2003. Redox signaling and the MAP kinase pathways. Biofactors 17, 287–296.

Yang, J.Y., Michod, D., Walicki, J., Widmann, C., 2004. Surviving the kiss of death. Biochemical Pharmacology 68, 1027–1031.